IEEE Access
Multidisciplinary | Rapid Review | Open Access Journal

Received September 5, 2019, accepted September 23, 2019, date of publication September 27, 2019,
date of current version October 8, 2019.

Digital Object Identifier 10.1109/ACCESS.2019.2944195

Probabilistic Short-Circuit Current in Active Distribution Networks Considering Low Voltage Ride-Through of Photovoltaic Generation

WEIYAN QIAN[1], NIANCHENG ZHOU[1], (Member, IEEE), JIAFANG WU[1], YUZE LI[1], QIANGGANG WANG[1], (Member, IEEE), AND PAN GUO[2]

[1]State Key Laboratory of Power Transmission Equipment and System Security and New Technology, Chongqing University, Chongqing 400044, China
[2]School of Physics and Electronic Engineering, Chongqing Normal University, Chongqing 401331, China

Corresponding author: Weiyan Qian (857254810@qq.com)

This work was supported by the National Natural Science Foundation of China under Grant 51577018.

ABSTRACT The probabilistic short-circuit current (PSCC) of photovoltaic generation is determined by the voltage sag at the grid connection and the low voltage ride-through of the unit during the grid fault, while the voltage sag and the low voltage ride-through are both stochastic. According to short-circuit current characteristics and Thevenin equivalent circuit in the transient state, this paper analyzes the changing trajectory of the equivalent internal potential of photovoltaic generation during the period of low voltage ride-through. To deal with the uncertainty of low voltage ride-through, the probability density function by the maximum entropy method is used to characterize the stochastic process of low voltage disconnection of photovoltaic generation. Based on the fault information, the calculation method of PSCC in active distribution network considering the uncertainty of low voltage ride-through of photovoltaic generation is proposed. Two cases of 9-node and 34-node distribution network are used to verify the effectiveness of the method. The obtained PSCC results can reasonably reflect the actual short-circuit current level of the active distribution network.

INDEX TERMS Photovoltaic, probabilistic short-circuit current, low voltage ride-through, active distribution network.

I. INTRODUCTION

The distributed photovaltaic generation has advatanges of clean and efficient. It can be used nearby and be adjusted by the different environment. In recent years, the installed capacity of photovoltaic generation in the distribution network has been expanding continuously [1], [2]. The technical specification for grid-connection of distributed generation requires that in case of grid failure, photovoltaic generation should maintain low voltage ride-through operation, and meanwhile give priority to providing reactive current support to the grid [3]–[5]. When voltage sag occurs at the grid connection point of photovoltaic generation, it is required to keep in safe operation with the requirement of low voltage ride-through. The injected short-circuit current is jointly determined by voltage sag at the grid connection and control of low voltage ride-through [6], [7].When the grid-connected voltage sags seriously, the photovoltaic generation is allowed to exit operation, and at this time, the photovoltaic generation has no short-circuit current injected into the grid [5]. Low voltage ride-through modeling of photovoltaic generation is a typical gray box problem. Different manufacturers and models of photovoltaic inverters have different topological structures, control strategies and parameters, which leads to the fuzziness of photovoltaic generation's low voltage ride-through ability [8]. At the same time, the random factors of grid faults lead to the randomness of voltage sag of grid points in the photovoltaic generation, which makes the short-circuit current during the fault of photovoltaic generation appear to be uncertain. Therefore, it is of great significance to evaluate the random variation range and distribution of probabilistic short-circuit current (PSCC) in active distribution network of distributed photovoltaic generation.

There are a large number of uncertainties in the calculation of short-circuit currents in power systems with distributed photovoltaic generation, such as fluctuations in photovoltaic

The associate editor coordinating the review of this manuscript and approving it for publication was Ahmed F. Zobaa.

generation output and random failure of system components such as generators, transformers and lines. If a deterministic short-circuit current calculation method is used to evaluate the impact of various uncertain factors on the system, it is necessary to make a large number of calculations based on various possible variations, which are computationally intensive and time-consuming. Therefore, this paper proposes a method for calculating the PSCC, which can consider the influence of uncertainty on the short-circuit current characteristics of the power system.

In terms of photovoltaic generation transient modeling, literature [9] studied the transient response characteristics of photovoltaic generation in linear and nonlinear regions and the influence law of control link. Literature [10] consider photovoltaic fault crossing control and established the steady short-circuit current calculation model, the literature [11] analyzed the photovoltaic effects of low voltage ride-through time sequences of short-circuit current. The above model only focuses on the steady-state short-circuit current of photovoltaic generation under different fault conditions, and the equivalent model of photovoltaic generation in the fault transient stage has not been studied. In terms of short-circuit current calculation, literature [12] puts forward the algorithm of short-circuit current in the radial distribution network considering the current-limiting characteristics of photovoltaic generation, while literature [11], [13]–[15] puts forward the calculation method of three-phase short-circuit current and asymmetric current which including photovoltaic generation based on the superposition principle. But those methods only focus on the calculation of certainty short-circuit current and do not consider the random factors such as system failure so that it does not calculate the uncertainty of photovoltaic power in the process of low voltage ride-through. They can only obtain the short-circuit current of the system in the worst case, and cannot obtain the change interval of the short-circuit current level of the system caused by the grid-connection of photovoltaic generation.

Calculations of PSCC provide comprehensive and rich information for power system planning and operation. Including the variation range and probability distribution of the short-circuit current of the fault point and different branches after the grid fault, and the probability that the system short-circuit current exceeds the breaker breaking capacity. These results help:

1) Obtain the contribution of renewable energy power generation to the system short-circuit current level more subtly, and provide reference for more reasonable determination of photovoltaic generation access schemes and system planning and design. In contrast, the deterministic short-circuit current calculation may make the short-circuit current level estimation insufficient, and the short-circuit current exceeds the circuit breaker interrupt current after the fault, which may harm the safe operation of the system; or the short-circuit current level may be estimated to be too high, resulting in unnecessary waste of equipment capacity.

2) PSCC is a tool for transient safety operation analysis of power systems with photovoltaic generation. It can more accurately and comprehensively evaluate the short-circuit current characteristics of the system. The calculation results can be used by the operators to analyze the weak links and potential risks of the system comprehensively, and help the operators to reasonably arrange the operation mode of the power system.

In terms of photovoltaic generation's low voltage ride-through, literature [16], [17] proposed an improved control strategy for photovoltaic generation based on positive and negative sequence compensation and model predictive control, so as to improve its control performance during grid failure. Literature [18]–[20] established the fault model of photovoltaic generation's low voltage ride-through through the test of photovoltaic inverters from different manufacturers and actual photovoltaic power stations. Literature [20] also analyzed the fault component characteristics of short-circuit current in the process of low voltage ride-through of photovoltaic generation. However, the previous literatures mainly modeled the current characteristics of photovoltaic generation in the process of low voltage ride-through, and the uncertainty of its low voltage ride-through ability has not been modeled in relevant literatures. At present, probabilistic methods have been applied to active distribution network voltage stability [21], voltage sag [22], power flow analysis [23] and other aspects. The probabilistic evaluation of short-circuit current level of active distribution network including distributed photovoltaic generation can be carried out by integrating random fault modeling, photovoltaic generation short-circuit current calculation and uncertainty modeling of low voltage ride-through.

Calculation of PSCC can account for various uncertainties in the power system, and is an important tool for the analysis of transient safety operation of power systems with photovoltaic generation. Therefore, this paper uses the uncertainty of photovoltaic power generation low voltage ride-through to establish a low voltage disconnection probabilistic model, and evaluates the PSCC of active distribution network. The main contributions of this paper are summarized as follows:

1) Considering the uncertainty of photovoltaic low voltage ride-through, analyzing the change trajectory of the transient internal potential, and establishing a random model of photovoltaic generation low voltage off- grid.

2) Combining the system fault information, the probabilistic method of the short-circuit current of the active distribution network is proposed to determine the distribution of the system PSCC.

3) The proposed method is verified by a certain 9-node and IEEE 34-node test systems, respectively.

The remainder of this paper is organized as follows. Second II builds the low voltage ride-through uncertain mode of photovoltaic generation. In section III, the distribution of the PSCC of photovoltaic generation is analyzed. The further analysis of the PSCC of distribution networks with photovoltaic generation is given in Section IV. Case studies are

presented in Section V, and Section Concludes summarizes the full paper.

II. UNCERTAINTY MODELING OF LOW VOLTAGE RIDE-THROUGH OF PHOTOVOLTAIC GENERATION

A. LOW VOLTAGE RIDE-THROUGH CONTROL OF PHOTOVOLTAIC GENERATION

Even if the voltage at the grid connection drops sharply, the photovoltaic generation will ride through the grid fault according to the grid-connected procedure [5], so photovoltaic generation system should have the ability of low voltage ride-through and provide reactive current support in the voltage sag process of the power grid.

As the core part of grid-connected photovoltaic generation, the inverter is also an important component to achieve low voltage ride through, which determines the output characteristics of photovoltaic generation without off-grid operation, its low voltage ride-through control block diagram is shown in Fig. 1. [24].

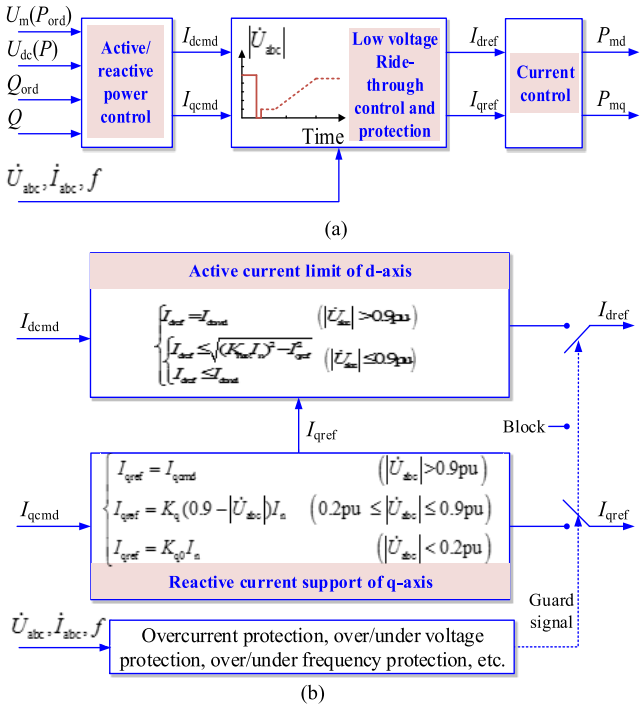

FIGURE 1. Requirements of photovoltaic generations low voltage ride-through. (a) Control and protection of photovoltaic inverters low voltage ride-through. (b) Control and protection of Low voltage ride-through unit.

According to Fig. 1(a), the inverter control protection includes three parts: active/reactive power control, low voltage ride-through control and protection, and current control. Where, U_m and U_{dc} are the maximum power point voltage of photovoltaic array and the DC side voltage of inverter respectively P, Q, P_{ord} and Q_{ord} represent the active and reactive power output of the inverter and the active and reactive power control instructions of the inverter respectively. After the active/reactive control link, the active control command current I_{dcmd} and reactive control command current I_{qcmd} are output. Then, the collected three-phase voltage phasor $\dot{U}_{abc}$, current phasor $\dot{I}_{abc}$ and network side frequency f on the AC side of the inverter are fed back to the fault ride-through control and protection link at the same time, and the reference values I_{dref} of d axis and I_{qref} of q axis component of the AC side of the inverter are calculated. Finally, through the current control link, the modulation ratio of the inverter PWM module to the d-axis component P_{md} and the q-axis component P_{mq} in the synchronous rotation dq coordinate system is obtained.

Fig. 1(b) is a detailed control block diagram of low voltage ride-through control and protection unit, which describes the transient characteristics of the inverter in the process of power grid fault and recovery, as well as the over/under voltage, over/under frequency and over current protection characteristics of the inverter. According to the requirements of literature [5], photovoltaic generation system should have the ability of low voltage ride-through and provide reactive current support in the voltage drop process of the power grid. It is according to the difference of the level of sags of inverter AC three-phase voltage $|U_{abc}|$. Firstly, determining the inverter AC q-axis component reference I_{qref} of AC side of inverter, provides reactive current for power grids, and on the basis of I_{qref} to determine the reference current of d-axis component I_{dref} and limit the active current. Where, K_{max} is the maximum current output multiple, K_{q0} and K_q are respectively the support coefficient of the inverter's zero-voltage ride-through and low voltage ride-through reactive current, and I_n represents the rated current of the inverter's ac side.

It can be seen from Fig. 1(a) that the protection control is closely related to the low voltage ride-through curve. When the terminal voltage falls and lasts for a period of time, photovoltaic power generation is likely to be off-line, and then change its output current and system short-circuit level.

B. LOW VOLTAGE RIDE-THROUGH UNCERTAIN REGION OF PHOTOVOLTAIC GENERATION

The low voltage ride-through curve (LVRTC) of photovoltaic generation is shown in the red curve in Fig. 1, where the horizontal axis represents the duration of voltage sag and the vertical axis represents the voltage amplitude. When the power grid fails, the voltage sag at the end of photovoltaic generation and the duration jointly determine whether the grid is off or not. If it is below LVRTC, i.e. in the blue area, photovoltaic generation will be withdrawn from the grid. Otherwise, it is in the state of grid-connected operation. Since more attention is paid to the short-circuit current at the initial stage of the fault when the power grid fails, and the fault clearance time is usually within 0.4s [25], this paper only considers the operation of photovoltaic generation within 0.4s.

The State Grid Electric Power Research Institute conducted a manual short-circuit test on the photovoltaic power station of Qinghai Power Grid. The waveform of the test results is shown in Fig. 2. It contains two Emerson SSL0500 inverters, one SUNGROW SG 500KTL inverter

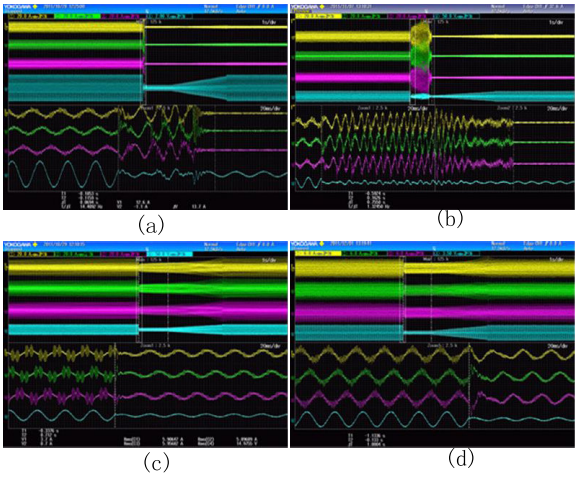

FIGURE 2. The waveform of the test results. (a)Emerson SSL0500-1. (b) Emerson SSL0500-2 (c)SUNGROW SG 500KTL (d) NR ELECTRIC PCS-9563-500kW.

and one NR ELECTRIC PCS-9563-500kW inverter. The different green symbols in Fig. 3 indicate the test results. It can be seen from the figure that the SSL0500 inverter corresponds to two test results, one of which has been off-grid at 0.07s after the terminal voltage drops to 0.2 pu, while the other was off the net after 0.75s.

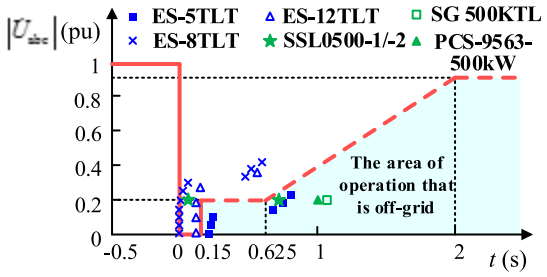

FIGURE 3. LVRTC and experimental results of photovoltaic generations.

Using the ACLT-1100 photovoltaic low voltage ride-through test device of Qunling Energy Resources [26] to carry out low voltage ride-through ability test on Warwick Energy ES-5TLT, ES-8TLT and ES-12TLT three small-capacity PV inverters, 5kW, 8kW and 12kW respectively. The detection was carried out under two working conditions, the output power of photovoltaic generation was 0.1pu $\sim$ 0.3pu and no less than 0.7pu, and repeating once at the same voltage sag test point. The average value of the test data of the two photovoltaic inverters was taken, and the test results were marked in Fig. 3 with different symbols.

According to the requirements of low voltage ride-through in literature [5], when the voltage of photovoltaic parallel grid drops to 0, it shall ensure continuous operation of 0.15s without disconnection. According to Fig. 3, the test results of both inverters do not fall strictly on the standard curve.

Therefore, it can be considered that in actual operation, the low voltage ride-through ability of each inverter is not the same because of the different types and sizes of inverters and the differences in the manufacturing industry of various manufacturers. Taking the above situations into consideration, it is approximately considered that it fluctuates in the region near the national standard curve, thus forming an uncertain region as shown in Fig. 4.

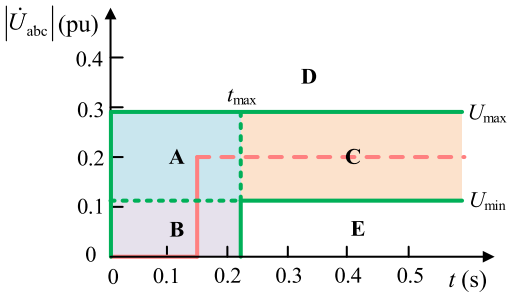

FIGURE 4. Uncertainty region of LVRTC.

The red curve in the Fig. 4 is the first half of the LVRTC. The green solid enveloping area is the uncertainty area defined in this paper. It is necessary to determine the position of the two green solid lines to obtain the range of the uncertainty area. Since the low voltage ride-through capability of different types of inverters is different, it is necessary to test multiple inverters, and the above range of the area is determined by the test data. The following two types of test results of the inverter are analyzed.

Low voltage ride-through capability test is carried out on multiple inverters. Some of the inverters can remain in the safe operating state for a certain period of time when the terminal voltage drops to 0 pu (Similar to the ES-5TLT inverter). Then t_{max} and U_{min} determines the lower boundary of the region. Where t_{max} represents the maximum time that the terminal voltage can remain in the safe operating state when the terminal voltage drops to 0 pu in the test results of multiple inverters, and U_{min} represents the minimum terminal voltage when the safe operating time greater than t_{max}. In another case, some inverters are off-grid when the terminal voltage has not dropped to 0 pu (Similar to the ES-8TLT inverter). At this time, U_{max} determines the upper boundary of the area, and U_{max} represents the maximum terminal voltage that can remain in the safe operating state in the test results of multiple inverters.

According to the Fig. 4, region D ($U > U_{max}$ part) is the operation area without disconnection. Area E ($U < U_{min}$ and $t > t_{max}$) is the off-grid operation area. The area enclosed by the solid green line ($U_{min} < U < U_{max}$ and $t < t_{max}$) is the uncertain area. For the convenience of analysis, the uncertain region is divided into three sub-regions, ABC, where B and C are the one-dimensional functions of t and U, and A is the two-dimensional functions of t and U. The uncertainty area of different types of inverters is different, and the variation range is determined by the test data.

C. PROBABILISTIC MODEL OF LOW VOLTAGE DISCONNECTION OF PHOTOVOLTAIC GENERATION

Whether or not photovoltaic generation is off-grid depends on the extent and duration of voltage sag. When voltage sag occurs in the uncertain region of LVRTC, the uncertainty of equipment on the extent and duration of voltage sag can be considered as epitaxial uncertainty, so it can be described by fuzzy variables. Due to the influence of manufacturers, equipment models, operating environment and other factors, the probability of photovoltaic disconnection in the region ABC is uncertain, t and U are both random variables. Assume the probability density functions of random variables t and U in region B and C be $f_x(t)$ and $f_y(U)$, respectively. Since t and U are two independent random variables, their product can be used to describe the random distribution rules in the uncertain region, so as to establish the off-grid random model.

In this paper, the probability density functions of random variables t and U are determined by the maximum entropy method based on the related studies on the severity and maximum entropy evaluation of voltage sag [28]. The mathematical model of probability density function can be expressed as

$$\text{Max } H_f = -\int_S f(t,U)\ln f(t,U)d(t,U) \tag{1}$$

$$\text{s.t.} \int_S f(t,U)d(t,U) = 1 \tag{2}$$

$$\int_S (t,U)f(t,U)d(t,U) = E_1 \tag{3}$$

$$\int_S [(t,U)-E_1]^n f(t,U)d(t,U) = E_n, \quad n = 2,3,\cdots,N \tag{4}$$

In these equations, H_f is the entropy of random variable (t,U), $f(t,U)$ is the probability density function of (t,U), S is the boundary of (t,U), E_1 and E_n are the first-order origin moment and n-order central moment of sample data of voltage sag degree.

The analytic expression of probability density function can be obtained by classical partial differentiation method, and Lagrange operator is introduced to model (1) ~ (4):

$$f(t,U) = \exp\{\lambda_0 + \lambda_1 s + \sum_{n=2}^{N}\lambda_i[(t,U)-E_1]^n\} \tag{5}$$

In this equation, $\lambda_i (i = 2,3,\ldots,N)$ is the Lagrange operator corresponding to the first-order moment constraint condition, and N = 5 [28] is often taken in practical projects.

In this paper, it is assumed that the probability density functions of random variables t and U obtained are equivalent to the evenly distributed probability density functions in probability theory, so

$$f(U) = \begin{cases} \dfrac{1}{U_{\max}-U_{\min}}, & U_{\min} < U < U_{\max} \\ 0, & \text{others} \end{cases} \tag{6}$$

$$f(\text{t}) = \begin{cases} \dfrac{1}{t_{\max}}, & 0 < t < t_{\max} \\ 0, & \text{others} \end{cases} \tag{7}$$

Since t and U are two independent random variables, $f_{x,y}(t,U) = f_x(t)f_y(U)$ can represent the joint probability density function of the random variables t and U in region A. By combining equations (6) and (7), the probability density function in the whole uncertain region can be obtained.

Assuming the PV terminal voltage sag has five situations $s_1 \sim s_5$, which are located in the ABCDE region, as shown in Fig. 5. Where s_1 is located in region D, photovoltaic maintains grid-connected operation, and short circuit current is injected into the grid, the off-grid probability is 0. Where s_1 is located in region D, photovoltaic maintains grid-connected operation, and short circuit current is injected into the grid, the off-grid probability is 0. U_3 and t_3 are voltage sags amplitude and duration of s_3, respectively. t_4 is the voltage sag duration of s_4; U_5 is the voltage sag amplitude of s_5.

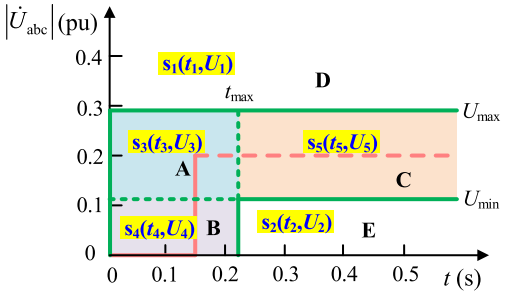

FIGURE 5. Evaluation of off-grid operation for photovoltaic generations.

When $s_1 \sim s_5$ occurs, the PV off-grid probability is respectively expressed as

$$\begin{cases} P_{s_1}(U_{\max} \le U) = 0 & (U_{\max} \ge U) \\ P_{s_2}(t_{\max} \le t, U \le U_{\min}) = 1 & (t \ge t_{\max}, U_{\max} \ge U) \\ P_{s_3}(0 \le t \le t_3, U_3 \le U \le U_{\max}) & \\ = \int_0^{t_3}\int_{U_3}^{U_{\max}} f_{x,y}(t,U)\,\mathrm{d}u\mathrm{d}t & \\ \qquad (t_{\max} \ge t, U_{\max} \ge U \ge U_{\min}) & \\ P_{s_4}(0 \le t \le t_4) = \int_0^{t_4} f_x(t)\,\mathrm{d}t & (t_{\max} \ge t, U_{\min} \ge U) \\ P_{s_5}(U_5 \le U \le U_{\max}) = \int_{U_5}^{U_{\max}} f_y(U)\,\mathrm{d}u & \\ \qquad (t_{\max} \ge t, U_{\max} \ge U \ge U_{\min}) & \end{cases} \tag{8}$$

The off-grid probabilistic model can be obtained by substituting equations (6) to (7):

$$\begin{cases} P_{s_1}(U_{max} \le U) = 0 & (U_{max} \ge U) \\ P_{s_2}(t_{max} \le t, U \le U_{min}) = 1 & (t \ge t_{max}, U_{max} \ge U) \\ P_{s_3}(0 \le t \le t_3, U_3 \le U \le U_{max}) & \\ = \dfrac{t_3(U_{max} - U_3)}{t_{max}(U_{max} - U_{min})} & (t_{max} \ge t, U_{max} \ge U \ge U_{min}) \\ P_{s_4}(0 \le t \le t_4) = \dfrac{t}{t_{max}} & (t_{max} \ge t, U_{min} \ge U) \\ P_{s_5}(U_5 \le U \le U_{max}) & \\ = \dfrac{U_{max} - U_5}{U_{max} - U_{min}} & (t_{max} \ge t, U_{max} \ge U \ge U_{min}) \end{cases} \tag{9}$$

This paper only takes photovoltaic generation as an example to analyze its uncertain region and off-grid probabilistic model. This idea is still applicable to the analysis of other distributed power sources.

III. PSCC INJECTED BY PHOTOVOLTAIC GENERATION

A. ANALYSIS OF STEADY-STATE FAULT CHARACTERISTICS OF PHOTOVOLTAIC GENERATION

Photovoltaic is a type of variable current power supply, which presents current limiting characteristics in the stage of power grid failure [7]. The reference value of current output on the ac side of the inverter is limited. According to drop level of the three-phase voltage $|U_{abc}|$ on the AC-side of the inverter, the reference value of current under different drop degrees is determined, and the current characteristics of photovoltaic generation under different terminal voltage sag are analyzed from this starting point.

Firstly, the reference value I_{qref} of ac side current q axis component of the inverter is determined according to equation (10). Where $I_{qref} = I_{qcmd} = 0$, $K_q = 1.5$, $K_{q0} = 1.05$ [5]. Reference value of d axis component of inverter ac side current I_{dref} is determined by equation (11). I_{dcmd} is related to the ratio of active power P to voltage $|U_{abc}|$, $I_{dcmd} = P/|U_{abc}|$. Assuming the PV runs at $P = 0.8$pu, $K_{max} = 1.5$. According to equation (11), the support of reactive current Iqref will have a certain impact on the output of active current.

$$\begin{cases} I_{qref} = I_{qcmd} & \left(\left|\dot{U}_{abc}\right| > 0.9\text{pu}\right) \\ I_{qref} = K_q\left(0.9 - \left|\dot{U}_{abc}\right|\right) I_n & \left(0.2\text{pu} \le \left|\dot{U}_{abc}\right| \le 0.9\text{pu}\right) \\ I_{qref} = K_{q0} I_n & \left(\left|\dot{U}_{abc}\right| < 0.2\text{pu}\right) \end{cases} \tag{10}$$

$$\begin{cases} I_{dref} = I_{dcmd} & \left(\left|\dot{U}_{abc}\right| > 0.9\text{pu}\right) \\ \begin{cases} I_{dref} \le \sqrt{(K_{max} I_n)^2 - I_{qref}^2} \\ I_{dref} \le I_{dcmd} \end{cases} & \left(\left|\dot{U}_{abc}\right| \le 0.9\text{pu}\right) \end{cases} \tag{11}$$

The variation trend of I_{qref}, I_{dref} and I_{ref} with terminal voltage is drawn respectively, as shown in Fig. 6(a). In the figure, I_{qref} increases proportionally with terminal voltage sag and tends to be constant. However, I_{dref} is limited as the terminal voltage sag gradually increases to the extreme value. I_{dref} gradually decreases and finally reaches a constant value because of the increase of reactive current. I_{ref} is the instruction value of total current, $I_{ref} = \sqrt{I_{dref}^2 + I_{qref}^2}$ which is similar to the output current of photovoltaic generation. As the terminal voltage sag gradually increases, the amplitude limiting output when it reaches 1.5pu.

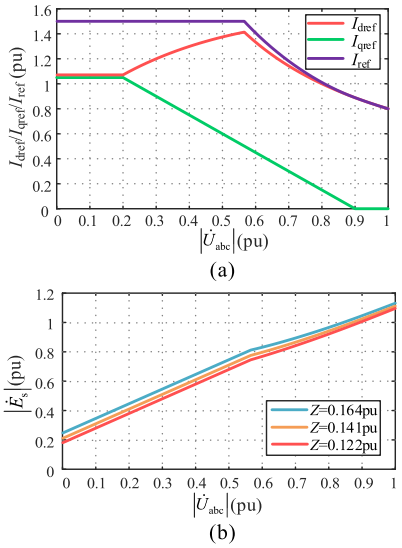

FIGURE 6. Variation ranges of Iqref, Idref, Iref and Es: (a) Iqref, Idref and Iref, (b) Es.

Thevenin equivalent circuit can represent the photovoltaic generation port. $\dot{E}_s = Z \cdot \dot{I}_{abc} + \dot{U}_{abc}$, $\dot{E}_s$ is the equivalent internal potential, Z is the virtual control impedance, whose size is determined by the control parameters [6]. The measured virtual control impedance values are substituted into the above equation to draw the variation trend of internal potential $|E_s|$ with terminal voltage $|U_{abc}|$ as shown in Fig. 6(b). It can be seen from the figure that the internal potential $|E_s|$ presents two changing trends. When the current limit is not entered, $|E_s|$ decreases slowly with $|U_{abc}|$; when the output current is limited, the current remains constant, and $|E_s|$ decreases proportionally but is still slightly larger than the terminal voltage $|U_{abc}|$.

B. ANALYSIS OF PHOTOVOLTAIC GENERATION FAULT TRANSIENT PROCESS

The above analysis is based on the steady-state stage of short-circuit current, but in actual faults, the short-circuit current needs to go through a transient process to finally transition to the steady state [9]. When the terminal voltage $|U_{abc}|$ drops to 0.72pu, the transient process of photovoltaic short-circuit current is shown in Fig. 7(a). For the purpose of discussion, point A in the figure is defined as the fault occurrence point, point B as the rise point of short-circuit current transient, point C as the maximum point of short-circuit current transient, and point D as the steady-state point of short-circuit current.

Since the equivalent expression of the photovoltaic generation port is based on the fault transient analysis, and the

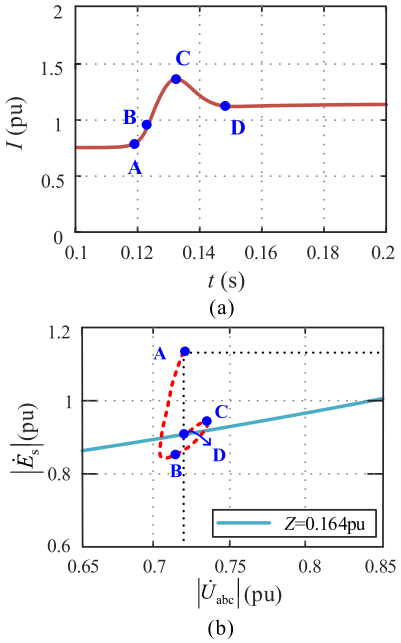

FIGURE 7. Transient process of short-circuit current and $|\dot{E}_S|$. (a) Transient process of short-circuit current. (b) Change track of $|\dot{E}_S|$.

curve of $|E_s|$ in Fig. 6(b) is calculated by the steady-state short-circuit current, the electric potential $|E_s|$ in the fault transient stage does not change in strict accordance with the curve in Fig. 6(b). But it can be considered that the trend of the two is roughly the same. In this paper, the four representative short-circuit current transient values of ABCD are put into equation $\dot{E}_s = Z \cdot \dot{I}_{abc} + \dot{U}_{abc}$ to backstepping the change trajectory of $|E_s|$, as shown in Fig. 7(b).

The red dotted line in Fig. 7(b) represents the change trajectory of the potential $|E_s|$ when the terminal voltage sags to 0.72pu. The blue curve is the variation trend of $|E_s|$ when the virtual impedance $Z = 0.164$pu in Fig. 6(b).Four points of ABCD in the figure correspond to those in Fig. 7(a). Point A is the initial value of $|E_s|$, and $|E_s|$ is considered to remain unchanged at the moment of failure. After the fault, the voltage sag is large, and the current response needs a certain time. According to equation $\dot{E}_s = Z \cdot \dot{I}_{abc} + \dot{U}_{abc}$, the internal potential cannot maintain the original value, so $|E_s|$ keeps decreasing and reaches the lowest point. Then the short-circuit current flows through the control output in a transient upward trend, and $|E_s|$ will gradually increase and pass through point B, which is slightly lower than the steady-state value and lies below the blue curve. When the current reaches the maximum, $|E_s|$ also reaches the maximum, that is the point C in the Fig. 7(a). At this moment, $|E_s|$ is temporarily higher than the steady state value and above the blue curve. Finally, the current transfers to the steady-state stage of short circuit, and $|E_s|$ also falls back to the steady-state point D on the blue curve. It can be seen from the above analysis that, in the process of fault transient, the internal potential $|E_s|$ is similar to the short-circuit current, both of which have a transient change process and eventually return to the steady-state value.

C. THREE-PHASE SHORT-CIRCUIT FAULT PROCESS ANALYSIS OF PHOTOVOLTAIC POWER DISTRIBUTION NETWORK

In case of failure of the grid containing photovoltaic generation, the photovoltaic generation system has the ability of low voltage ride-through, and even if the voltage at the grid points drops significantly, the photovoltaic generation will still operate in accordance with the grid connection rules [5], and provide reactive current support during the voltage drop process of the grid. However, when the terminal voltage falls and lasts for a period of time, photovoltaic generation is likely to be off-grid, which will change its output current and system short-circuit level.

When multiple photovoltaic generation systems are connected to the grid, the off-grid time of each system is inconsistent, which leads to the change of fault current at the short circuit and shows that the fault current decreases with the diconnection of the photovoltaic system. As shown in Fig. 8(a), taking the three-phase short-circuit fault of accessing three photovoltaic systems as an example. When a photovoltaic system is off-grid, no fault current is provided to the fault point, so the fault current at the fault point decreases until all the photovoltaic system is off-grid. Then the fault current is only provided by the grid, as shown in Fig. 8(b) red line.

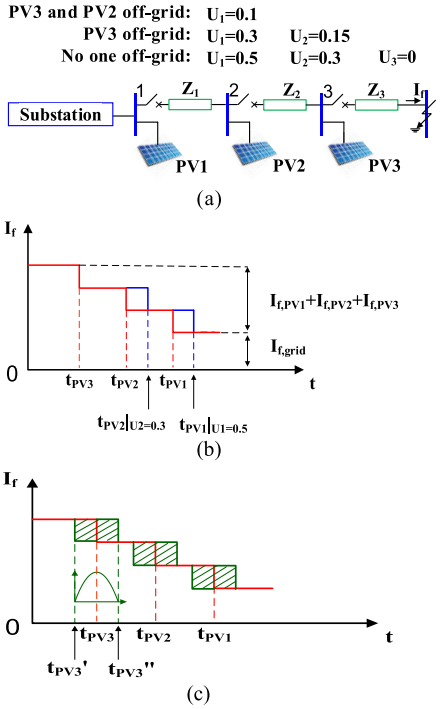

FIGURE 8. Failure process of distribution network with PV. (a) A system with 3 PV. (b) The fault current provided by PV. (c) Off-grid uncertain area.

As the voltage of feeder will change after the photovoltaic system is off-grid, so will the off-grid time. The blue line in

Fig. 8(b) shows the off-grid situation of PV2 and PV1 when the voltage does not change.

As whether the photovoltaic generation is off-grid is determined by the extent and duration of voltage drop at the end, when the voltage sag occurs in the uncertain region of LVRTC, there is uncertainty about whether the equipment is off-grid. The off-grid time of each pv system is uncertain. In Fig. 8(c), the green shaded part represents the off-grid uncertain area. Taking PV3 as an example, PV3 disconnection may occur within the uncertain time interval $[t_{PV3}', t_{PV3}'']$, resulting in the change of fault current.

Therefore, when conducting fault process analysis of photovoltaic power distribution network, it is necessary to consider the off-grid probability of photovoltaic system and analyze its uncertainty region and off-grid probabilistic model to expand the traditional fault analysis method.

IV. CALCULATION METHOD OF PSCC IN DISTRIBUTION NETWORKS WITH PHOTOVOLTAIC GENERATION

In the photovoltaic distribution system, each feeder may fail, and the fault location and fault type are random. In addition, each photovoltaic generation may be off-grid during the fault period, so it will have a certain impact on the short-circuit current of the system.

In order to comprehensively evaluate the short-circuit current of the system, in addition to the photovoltaic generation low voltage off-grid probabilistic model proposed above, a series of uncertain factors including fault lines, fault types and fault duration in the system should also be comprehensively considered.

Without loss of generality, it can be considered that the failure rate of each line is proportional to its length, and the failure probability of each point on a certain line is the same, that is, it obeyes to the uniform distribution of [0,1]. Considering that there are four types of faults, namely single-phase grounding fault (LG), two-phase phase-to-phase fault (2L), two-phase grounding fault (2LG) and three-phase fault (3L), it is necessary to carry out statistical analysis of distribution network faults to obtain the occurrence probability of various types of faults. In practice, it is difficult to obtain real data, so it is assumed that the occurrence probability of various faults in the network is the same as that in literature [29], as shown in Tab. 1.

TABLE 1. Probability of each fault type.

Fault type	Probability
LG	0.72
2L	0.05
2LG	0.2
3L	0.03

According to the Technical requirements for connecting photovoltaic power station power system [5], when different types of faults occur, the selection of the evaluation voltage is different, as shown in Tab. 2.

TABLE 2. Evaluation voltage for LVRT of PV stations.

Fault type	Evaluation voltage
LG	Phase voltage
2L	Line voltage
2LG	Phase voltage
3L	Line voltage

When performing the analysis of the PSCC, the fault type should be determined firstly, and then selecting the corresponding evaluation voltage. Fault duration and relay protection device type and duration of action are concerned, this article assumes that the fault duration obey the expectations of 0.18s, the standard deviation of 0.06s normal distribution, and the fault transition impedance obedience expected for the 5Ω normal distribution of the standard deviation of 1Ω [22].

Monte carlo method can be used to deal with random problems of multidimensional complex systems [22]. Random sampling of the above uncertain factors is carried out to obtain the value of random variables, and then iterative calculation is carried out. The PSCC is further carried out by combining the low voltage off-grid probability model of photovoltaic generation. The specific flow chart is shown in Fig. 9.

The procedure is mainly carried out in the following steps: (1) Firstly, the sampling frequency is set, and according to the distribution characteristics of fault events, the fault line, fault location, fault type, fault duration and other fault information are acquired by random sampling. (2) Determining the evaluation voltage by the type of failure. (3) Calculate the voltage drop degree and the maximum photovoltaic output current I_{pvn} in case of failure of photovoltaic parallel grid terminal by the nth sampling value.(4) In combination with the photovoltaic low voltage off-grid probability model in section 2 of this paper, the off-grid probability P_{pvn} of photovoltaic generation in the nth sampling is obtained according to the voltage sag degree and duration, and then the expected value of photovoltaic generation injection current $(1\text{-}P_{pvn}) \cdot I_{pvn}$ is calculated.(5) Put the expected value into the short circuit calculation program to calculate the short circuit current at the fault point.(6) After n times of sampling, the short-circuit current values of fault points under different fault conditions are obtained, and the probability distribution diagram of short-circuit current is finally formed.

V. CASE STUDY

This paper takes the 9-node structural parameters of the actual grid in a certain area of Fujian and the parameters of IEEE 34 Node Test Feeder as examples. The simulation model is built in MATLAB/Simulink, and use the method of this article to obtain the distribution of PSCC of the grid under photovoltaic generation. Since the influence of load on the calculation of short-circuit current is usually ignored

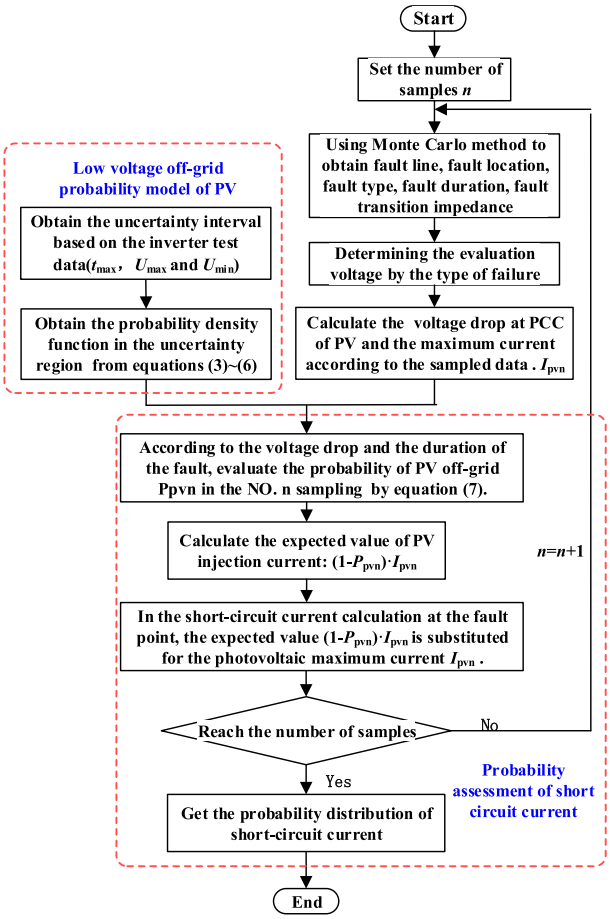

FIGURE 9. Flow chart of PSCC calculation.

in practical calculations, the following examples are calculated and simulated under the no-load condition before short-circuit.

In the example, each photovoltaic generation consists of 500kW photovoltaic generator units, the rated voltage of a single unit is 315V, the power factor is 1, and the unit parameters are shown in Tab. 3. The controllers adopt the low voltage ride through control and protection links specified in GB/T32826-2016, the voltage of inverter DC remains constant during grid faults, and the upper limit of the output current of a single PV inverter is 1.5 times the rated current. Considering that the photovoltaic generation output changes with the illumination fluctuation in actual operation, in the simulation, the light intensity of all photovoltaic generation inputs is 1000W/m^2, the input ambient temperature is 30°C, the output of photovoltaic generation is mainly determined by the light intensity.

TABLE 3. Basic parameters of photovoltaic generations.

Parameter	Value
Type	SG500MX-M
Rated AC output power	500kW
Rated frequency	50Hz
Maximum output voltage（VDC）	1000V
MPPT voltage range（VDC）	480~850V
Rated grid voltage（VAC）	315V
Maximum continuous operating current	1018A
Power factor	≥0.99

A. 9-NODE TEST CASE

The network structure of 10kV feeder line in a certain area of Fujian is shown in Fig. 10. Among them, node 2, node 3, and node 6 are respectively connected to 0.5MW, 1MW, and 1.5MW of photovoltaic generation, performing fault simulation on the line by MATLAB/Simulink.

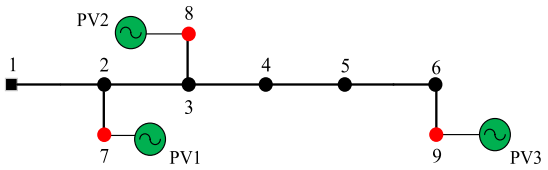

FIGURE 10. 9- node test system.

Firstly, to solve the off-grid probability model of photovoltaic generation. For easy calculation, this paper assumes that the U_{min}, U_{max} and t_{max} of all photovoltaic generation is 0.1pu, 0.3pu and 0.2s when tested in low voltage ride-through.

According to the method in Section 3 of the text, set the sampling number n to 500 times. It is obtained from Tab. 2: In the 500 times fault simulation, the single-phase grounding fault is 360 times, the two-phase grounding fault is 100 times, the two-phase phase-to-phase fault is 25 times, and the three-phase short-circuit fault is 15 times. Then select the evaluation voltage from Tab. 1. The following are the results obtained after the program is run 500 times.

The voltage sag of the photovoltaic grid-connected point (ie, nodes 7, 8, 9) is shown in Fig. 11. As can be seen from the figure, the probability that the voltage of the three photovoltaic generation terminals drops below 0.5pu is large, part of the photovoltaic generation may face disconnection, which will affect the system short-circuit current. Therefore, it is necessary to combine the voltage sag time to evaluate the system PSCC.

Taking the calculated voltage sag value of PV terminal by each sampling and the randomly generated fault duration into its low voltage off-grid probability model, the off-grid probability P_{pv} of each photovoltaic can be calculated, and then the expected value (1-P_{pv})·I_{pv} of the photovoltaic generation output current under this particular condition is obtained. Fig. 12 shows thedistribution results for the expected PSCC of each photovoltaic generation in the system after 500 samples.

It can be seen from the figure that the PSCC of each photovoltaic generation is expected to be 0 is higher, and PV4 is the most significant, this shows that in actual operation, PV is likely to face disconnection during the fault and the

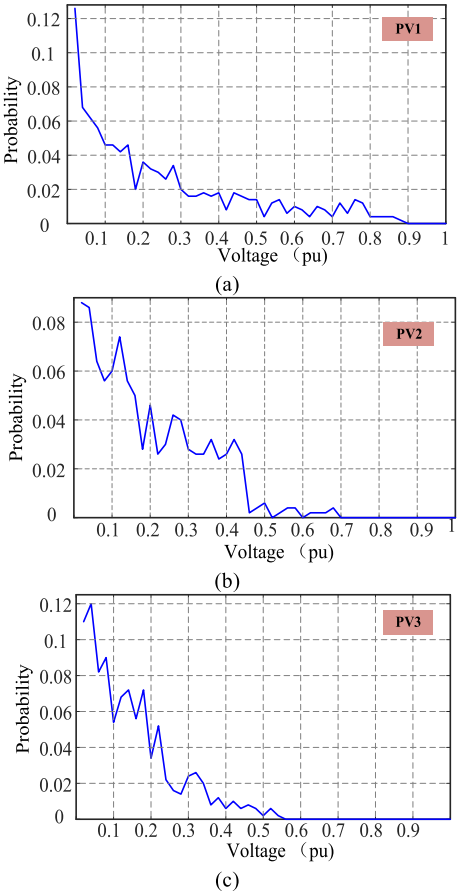

FIGURE 11. Probability distribution of voltage sag at grid-connected point of photovoltaic generations. (a) PV1. (b) PV2. (c) PV3.

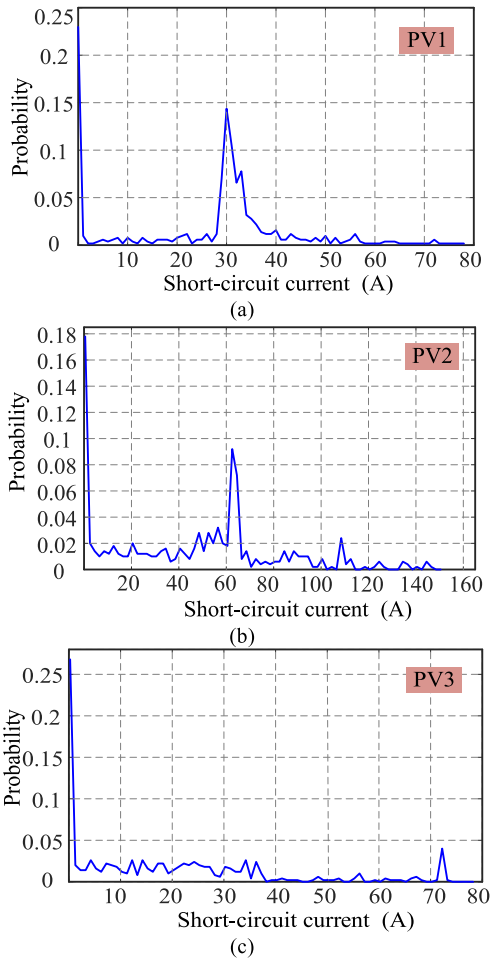

FIGURE 12. Distribution of expected value of PSCC of photovoltaic generations. (a) PV1. (b) PV2. (c) PV3.

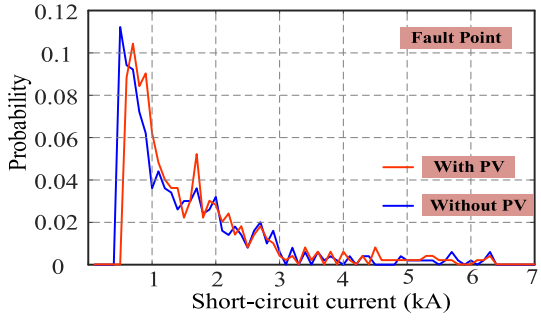

FIGURE 13. Distribution of PSCC at fault points.

output current is 0, which will affect the accurate evaluation of the short-circuit current at the fault point. Therefore, it is necessary to improve the current output result in combination with the actual disconnection of photovoltaics, and to reflect the operational status of photovoltaic generation during grid faults from an objective perspective. In addition, the expected PSCC of PV1 and PV2 at 30A and 60A also shows a higher trend, and the current magnitude is positively correlated with its capacity, the PV2 has a capacity twice that of PV1, so the short-circuit current is also twice.

Each sampling takes the expected value of each short-circuit current of photovoltaic generation into the short-circuit calculation program, and obtains the short-circuit current at fault point and the short-circuit current flowing through each node. The distribution of the PSCC obtained after 500 times of program operation is shown in Fig. 13 and Fig. 14. The red line and the blue line in Fig. 13 indicate the distribution results of the PSCC at the fault point without PV and with PV respectively. It can be seen from the figure that the blue line area is slightly to the left of the red line area, indicating that the access of the photovoltaic will increase the short circuit level of the system to some extent.

When PV is connected, the short-circuit current at the fault point can be as close as 6.5kA, but the PSCC appearing between 0.5kA and 1kA is greater. This is because the PSCC of a single-phase fault in the system is much greater than other fault types, and the short-circuit current generated by single-phase fault is the smallest. According to the distribution in Fig. 13, the system electrical equipment can be reasonably configured, such as determining the breaking capacity of the system breaker.

The statistical results of the short-circuit current flowing through the rest of the system in 500 sampling calculations

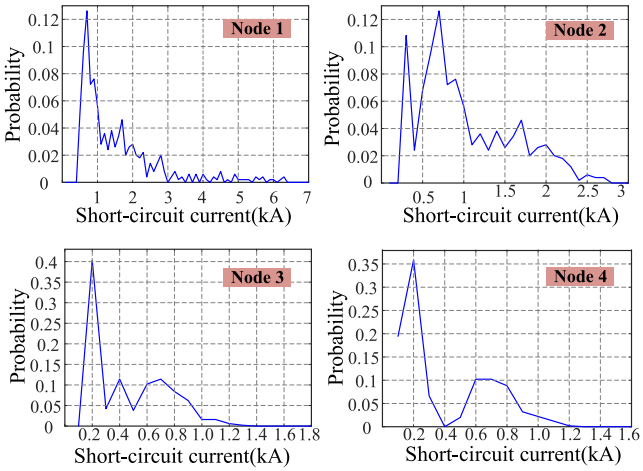

FIGURE 14. Distribution of PSCC at some nodes.

are shown in Fig. 14. The PSCC distribution flowing through node 1, node 2, node 3, and node 4 is listed in Fig. 14. As can be seen from the figure, the closer to the conventional power supply, the greater the short-circuit current flowing through the node. This is because the short-circuit capacity of the conventional power supply is much larger than that of photovoltaic generation, which plays a leading role in the magnitude of the short-circuit current.

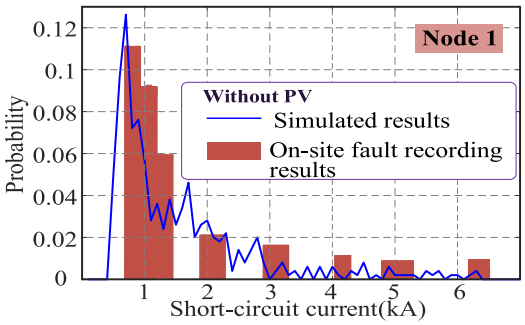

FIGURE 15. Comparison between simulation results and on-site fault recording resualt at node 1.

In order to illustrate the correctness of the method, a total of 53 sets of historical short-circuit current data of the substation (Node 1) of the power distribution system were collected, processed and plotted as a histogram, and compared with the simulation results of this paper, as shown in Fig. 15. The solid blue line in the figure represents the simulation results of the method, and the red histogram shows the distribution of the recorded data after processing. Because the acquired recording data is limited, and the fault conditions set by the simulation are different from the actual situation of the grid, the two are not completely coincident. However, it can be seen from the figure that the trends of the two are roughly the same, which indicates the method results have certain correctness and reference.

B. 34-NODE TEST CASE

The network structure of IEEE 34 Node Test Feeder is shown in Fig. 16. It is connected to 10 PV generator units, of which

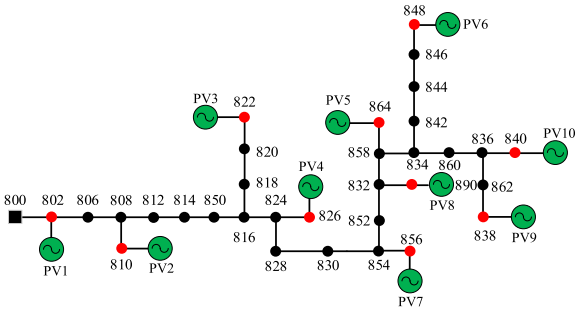

FIGURE 16. IEEE 34- node test system.

the red node is the PV power generation access point. The minimum PV access capacity is 0.5MW and the maximum is 1.5MW. Using the method of Section 3, the network is simulated 1000 times to obtain the distribution of the system PSCC. It is obtained from Tab. 2: In the 1000 times fault simulation, the single-phase grounding fault is 720 times, the two-phase grounding fault is 200 times, the two-phase phase-to-phase fault is 50 times, and the three-phase fault is 30 times. Then select the evaluation voltage from Tab. 1. Fig. 17 and Fig. 18 show the distribution of the PSCC at fault point and other nodes.

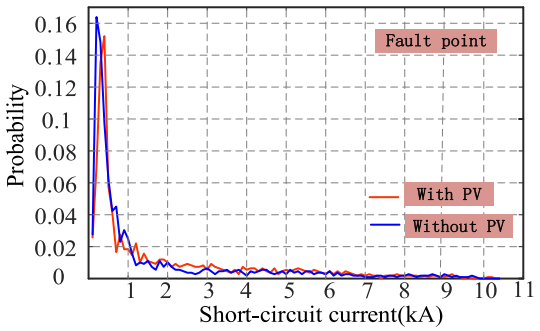

FIGURE 17. Distribution of PSCC at fault points.

The blue and red polylines in Fig. 17 respectively indicate the probability distribution results of the short-circuit current at the fault point when the photovoltaic is not connected and connected to the grid. It can be seen from the figure that the grid connection of photovoltaic generation will improve the short circuit level of the system to a certain extent. Moreover, the number of photovoltaic grids of the network is increased compared with the 9-node network, so the impact on the short-circuit current at the fault point is greater.

Comparing Fig. 17 with Fig. 18, it can be seen that since the short-circuit current at the fault point is provided by the conventional power source and the photovoltaic generation, the short-circuit current is the largest. And from the node 800 to the node away from the conventional power supply, the maximum short-circuit current and the maximum PSCC are reduced, and the short-circuit current provided by the conventional power source is much larger than that of the photovoltaic generation. It can be considered that the closer the node is to the conventional power supply, the greater the short-circuit current will be.

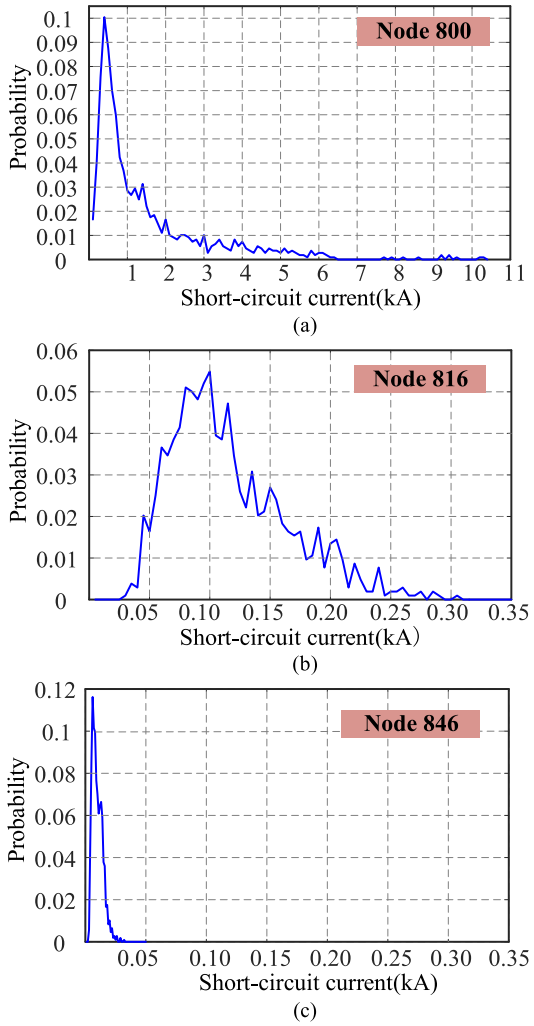

FIGURE 18. Distribution of PSCC at some nodes. (a) Node 800. (b) Node 816. (c) Node 846.

In addition, as can be seen from Fig. 18, the distributions of the PSCC of the nodes are different, wherein the distributions of the nodes 800 and 846 are concentrated, and the short-circuit current distribution of the nodes 8 is relatively dispersed. This is related to the overall topology of the system. The node 800 is located at the head end of the network and is connected to a conventional power source. The node 846 is in the middle of the network, and the adjacent nodes have grid-connected photovoltaics. The two are relatively single-effected by conventional power sources or photovoltaic generation, so the short-circuit current distribution is also more concentrated. In Fig. 16, the node 816 is in the middle of the network, and there are many connecting branches, which are affected by the common power supply and the photovoltaic generation, so the distribution of the short-circuit current is more dispersed. The method propoesd from this paper can not only evaluate the maximum short-circuit current of the system, but also obtain the probability interval of the short-circuit current and the maximum PSCC of the system, which has certain reference value for the reasonable configuration of the electrical equipment of the system.

VI. CONCLUSION

This paper is based on the short-circuit current characteristics of photovoltaic generation faults, combined with the Thevenin equivalent circuit to analyze the variation trend of the internal potential during the fault transient process, then consider the uncertainty of the low voltage ride-through curve, and combined with the system fault information, the calculation method of PSCC in active distribution network considering the uncertainty of low voltage ride-through of photovoltaic generation is further proposed. This paper reveals the effect of low voltage disconnection on system short-circuit current from the perspective of probability, compared with the precise calculation method under human specific conditions, the probability assessment is beneficial to present more objective results, comprehensively grasp the probability distribution of the system short-circuit current, and provide an effective basis for system equipment selection.

REFERENCES

[1] N. Mourad and B. Mohamed, "Impact of increased distributed photovoltaic generation on radial distribution networks," in *Proc. Int. Conf. Control, Decis. Inf. Technol. (CoDIT)*, St. Julian's, Malta, Apr. 2016, pp. 292–295.

[2] J. He, L. Liu, W. Li, and M. Zhang, "Development and research on integrated protection system based on redundant information analysis," *Protec. Control Modern Power Syst.*, vol. 1, no. 2, p. 13, 2016.

[3] K. Jia, C. Gu, Z. Xuan, L. Li, and Y. Lin, "Fault characteristics analysis and line protection design within a large-scale photovoltaic power plant," *IEEE Trans. Smart Grid*, vol. 9, no. 5, pp. 4099–4108, Sep. 2018.

[4] J. H. He, Y. H. Cheng, J. Hu, and H. T. Yip, "An accelerated adaptive overcurrent protection for distribution networks with high DG penetration," in *Proc. 13th Int. Conf. Develop. Power Syst. Protection (DPSP)*, Edinburgh, U.K., Mar. 2016, pp. 1–5.

[5] *Technical requirements for connecting photovoltaic power station to power system*, Standard GB/T 19964-2012, The State Administration of Quality Supervision, Inspection and Quarantine, China Standard Press, Beijing, China, 2013.

[6] L. V. Strezoski, M. D. Prica, V. A. Katic, and B. Dumnic, "Short-circuit modeling of inverter based distributed generators considering the FRT requirements," in *Proc. North Amer. Power Symp. (NAPS)*, Denver, CO, USA, Sep. 2016, pp. 1–6.

[7] H. Hooshyar and M. E. Baran, "Fault analysis on distribution feeders with high penetration of PV systems," *IEEE Trans. Power Syst.*, vol. 28, no. 3, pp. 2890–2896, Aug. 2013.

[8] L. Qu, T. Shi, M. Sun, and L. Zhu, "Study on low voltage ride through test methods for PV inverter," in *Proc. China Int. Conf. Electr. Distrib.*, Shanghai, China, Sep. 2012, pp. 1–5.

[9] X. Kong, Y. Yuan, P. Li, and Y. Wang, "Study on the fault current transient features of the PV inverter," in *Proc. Int. Conf. Renew. Power Gener. (RPG)*, Beijing, China, Oct. 2015, pp. 1–7.

[10] H. Zhao, N. Wu, S. Fan, Y. Gao, L. Liu, Z. Zhao, and X. Liu, "Research on low voltage ride through control of PV grid-connected inverter under unbalance fault," in *Proc. Chin. Automat. Congr. (CAC)*, Jinan, China, Oct. 2017, pp. 3991–3996.

[11] Q. Wang, N. Zhou, and L. Ye, "Fault analysis for distribution networks with current-controlled three-phase inverter-interfaced distributed generators," *IEEE Trans. Power Del.*, vol. 30, no. 3, pp. 1532–1542, Jun. 2015.

[12] C. A. Plet and T. C. Green, "A method of voltage limiting and distortion avoidance for islanded inverter-fed networks under fault," in *Proc. 14th Eur. Conf. Power Electron. Appl.*, Birmingham, U.K., Aug./Sep. 2011, pp. 1–8.

[13] Y. Liu, R. Yu, L. Zhang, D. Jiang, N. Chen, and D. Zhao, "Research on short-circuit currents calculation method considering dynamic reactive power support of renewable energy systems," in *Proc. 2nd IEEE Conf. Energy Internet Energy Syst. Integr. (EI2)*, Beijing, China, Oct. 2018, pp. 1–9.

[14] Z. Dai, C. Li, and X. Chen, "Fault model of IIDG considering LVRT and its application in fault analysis of active distribution networks," in *Proc. IEEE Region Conf. (TENCON)*, Singapore, Nov. 2016, pp. 3831–3834.

[15] H. Margossian, J. Sachau, and G. Deconinck, "Short circuit calculation in networks with a high share of inverter based distributed generation," in *Proc. IEEE 5th Int. Symp. Power Electron. Distrib. Gener. Syst. (PEDG)*, Galway, Ireland, Jun. 2014, pp. 1–5.

[16] E. Afshari, B. Farhangi, Y. Yang, and S. Farhangi, "A low-voltage ride-through control strategy for three-phase grid-connected PV systems," in *Proc. IEEE Power Energy Conf. Illinois (PECI)*, Champaign, IL, USA, Feb. 2017, pp. 1–6.

[17] J. Lihu, Z. Yongqiang, G. Wenrai, and W. Yinshun, "Application of model current predictive control in low voltage ride through of photovoltaic station," in *Proc. Int. Conf. Power Syst. Technol.*, Chengdu, China, Oct. 2014, pp. 2846–2851.

[18] M. Liu, J. Huang, Y. Dong, and H. Li, "Steady-state control performance modeling and simulation analysis for grid-connected PV inverter," in *Proc. China Int. Conf. Electr. Distrib. (CICED)*, Xi'an, China, Aug. 2016, pp. 1–4.

[19] Z. Fei, Z. Junjun, and D. Mingchang, "A novel voltage sag generator for low voltage ride-through testing of grid-connected PV system," in *Proc. IEEE Int. Conf. Comput. Sci. Automat. Eng. (CSAE)*, Zhangjiajie, China, May 2012, pp. 136–140.

[20] X. Bao, P. Tan, F. Zhuo, and X. Yue, "Low voltage ride through control strategy for high-power grid-connected photovoltaic inverter," in *Proc. 28th Annu. IEEE Appl. Power Electron. Conf. Exposit. (APEC)*, Long Beach, CA, USA, Mar. 2013, pp. 97–100.

[21] D. Z. Fang, L. Jing, and T. S. Chung, "Corrected transient energy function-based strategy for stability probability assessment of power systems," *IET Generation, Transmiss. Distribution*, vol. 2, no. 3, pp. 424–432, May 2008.

[22] D. Jia, "Study on evaluation of voltage sag exposed areas in large scale complex distribution network," in *Proc. Int. Conf. Cyber-Enabled Distrib. Comput. Knowl. Discovery (CyberC)*, Chengdu, China, Oct. 2016, pp. 459–464.

[23] R. Zhong, Y. Teng, X. Wang, Y. Zhu, and H. Zhang, "Probabilistic optimal power flow calculation of AC/DC hybrid distribution network with photovoltaic power and electric vehicles," in *Proc. Int. Conf. Power Syst. Technol. (POWERCON)*, Guangzhou, China, Nov. 2018, pp. 20–27.

[24] *IEEE Approved Draft Recommended Practice for Sizing Lead-Acid Batteries for Stand-Alone Photovoltaic (PV) Systems*, IEEE Standard P1013/D1.3, May 2019, pp. 1–54.

[25] Z. Zexin, S. Xiaofan, Z. Chunxia, W. Shirong, J. Yiguo, and D. Dingxiang, "Dynamic simulation inspection test for protection equipment in China," in *Proc. Int. Conf. Power Syst. Technol.*, Kunming, China, vol. 1, Oct. 2002, pp. 280–284.

[26] *IEEE Approved Draft Recommended Practice for Voltage Sag and Short Interruption Ride-Through Testing for end-use Electrical Equipment Rated Less than 1000 V*, IEEE Standard P1668/D2, Sep. 2016, pp. 1–89.

[27] H. Liu, Q. P. Huang, D. Yang, and X. Y. Xiao, "Equipment voltage sag sensitivity test and feature extraction," in *Proc. China Int. Conf. Electr. Distrib.*, Shanghai, China, Sep. 2012, pp. 1–4.

[28] X.-Y. Xiao, C. Ma, and H.-G. Yang, "Voltage sag assessment based on maximum entropy principle," in *Proc. 20th Int. Conf. Exhib. Electr. Distrib. (CIRED)*, Jun. 2009, pp. 1–5.

[29] S. K. Goswami and S. K. Basu, "A new algorithm for the reconfiguration of distribution feeders for loss minimization," *IEEE Trans. Power Del.*, vol. 7, no. 3, pp. 1484–1491, Jul. 1992.

WEIYAN QIAN received the B.S. degree in electrical engineering from Chongqing University, Chongqing, China, in 2018, where she is currently pursuing the M.S. degree. Her research interests include power system protection and control.

NIANCHENG ZHOU received the B.S., M.S., and Ph.D. degrees from Chongqing University, Chongqing, China, in 1991, 1994, and 1997, respectively. He was with Chongqing Kuayue Technology Company Ltd., from 1997 to 2003. He was a Research Fellow of Nanyang Technological University, Singapore, from 2010 to 2011. He is currently a Professor with the School of Electrical Engineering, Chongqing University. His research interests include the analysis and operation of power systems, microgrids, and power quality.

JIAFANG WU received the B.S. degree in electrical engineering from Hunan University, Hunan, China, in 2016, and the M.S. degree in electrical engineering from Chongqing University, Chongqing, China, in 2019. Her research interests include power system protection and control.

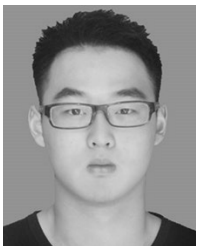

YUZE LI is currently pursuing the B.S. degree in electrical engineering from Chongqing University, Chongqing, China. His research interests include power system automation and power quality.

QIANGGANG WANG (S'13–M'15) received the B.S. and Ph.D. degrees from Chongqing University, Chongqing, China, in 2009 and 2015, respectively, where he has been a Lecturer with the School of Electrical Engineering, since 2015. He is currently a Research Fellow of Nanyang Technological University, Singapore. His research interests include power system operation, microgrids, and power quality.

PAN GUO received the B.S. and Ph.D. degrees from Chongqing University, Chongqing, China, in 2009 and 2015, respectively. She has been a Lecturer with the College of Physics and Electronic Engineering, Chongqing Normal University, China, since 2015. Her research interests include electrical new technology and nuclear magnetic resonance.